The current issue and full text archive of this journal is available at
www.emeraldinsight.com/0332-1649.htm

Analysis of the structure-dynamic behaviour of an induction machine with balancing kerfs

C. Schlensok
Bosch Rexroth AG, Lohr am Main, Germany, and
K. Hameyer
Institute of Electrical Machines, RWTH Aachen University, Aachen, Germany

Abstract

Purpose – To present results of research closely linked with real life applications. It resumes work of a period of about two years.

Design/methodology/approach – Applying the finite-element method (FEM) the impact of balancing kerfs in the bars of squirrel-cage rotors of a small scale, mass series induction machine (IM) is studied. For the analysis and design optimization of the IM both, 2D electromagnetic, multi-slice and 3D structure-dynamic models are considered. Introducing and applying a novel 2D-3D force-transformation scheme, all possible balancing variants of the IM are studied in terms of electromagnetic and mechanical behaviour.

Findings – The obtained results lead to a significant improvement of the studied IM. In fact, it is found, that the method of balancing the rotor by carving the rotor bars results in higher unbalanced pull rather than reducing it. This is due to electromagnetic unbalance caused by balancing. Hence, the IM is no longer balanced in series production. This again leads to a major economic benefit.

Research limitations/implications – Using the FEM for simulation of structure dynamic problems is often limited to how the boundary layers are handled. In real life materials are not "connected" but glued or clamped. Therefore, the behaviour can only be adopted by manipulating the material parameters derived from iterative parameter adoption by measurement.

Practical implications – Owing to the findings the IM is no longer balanced in series production, leading to a significant reduction of costs. In general, the applied methods can be used for the analysis and optimization of any kind of manufacturing or tolerance problem of electrical machines such as various kinds of eccentricity, punching kerfs, broken bars, magnetization errors in permanent-magnet machines, etc.

Originality/value – This contribution gives a close insight of how to study the impact of manufacturing and tolerance problems of electric machinery, applying the method to an IM with balancing kerfs.

Keywords Electric machines, Acoustics, Vibration, Finite element analysis, Induction machine, Harmonic analysis

Paper type Research paper

1. Introduction

1.1 General approach

For the analysis of the impact of manufacturing and tolerance problems in electrical machines a two-step chain of numeric models is applied as shown in Figure 1. With the finite-element method (FEM) electromagnetic and mechanical models are computed. The electromagnetic model consists of stator, winding, rotor, and air-gap and is excited by currents in the stator winding. Depending on the speed the rotor is moved in each simulation-time step applying the moving-band method (De Gersem *et al.*, 2006).

COMPEL: The International Journal for Computation and Mathematics in Electrical and Electronic Engineering
Vol. 27 No. 1, 2008
pp. 235-245

0332-1649
DOI 10.1108/03321640810836799

The electromagnetic model provides the flux-density distribution from which the net-force, the torque, and the surface-force density are derived. The latter is used as ex-citation for the succeeding mechanical model. This model consists of all mechanical parts as described later in the paper. It provides the deformation of the machine from which the body-sound is derived.

1.2 Concrete problem

Balancing rotating machine parts, for example, rotors of electrical machines, can be performed by various principles (Lingener, 1992). Depending on the mechanical part, its size, and the installation space either mass is added on the opposite side of the rotor's unbalance (e.g. balanced wheel rims on cars) or mass is removed at its location. This method is preferred for rotors of electrical machines. Here, an induction machine (IM) with squirrel-cage rotor is analysed balanced by removing mass. As Figure 2 shows, the mass is milled out of the iron of the rotor lamination on both ends of the IM. In the studied machine four neighbouring rotor teeth are affected on each end different from the prototype shown. The maximum tolerated length and width of the kerfs are shown in Figure 3. From the longitudinal section A_{kerf} of the kerf and the quadrangle A_{quad} the modified, effective length is derived:

$$\vec{l}_{\text{eff}} = \frac{A_{\text{kerf}}}{A_{\text{quad}}} = 12.74\,\text{mm} \approx 17\% \cdot l_{\text{Fe}}. \tag{1}$$

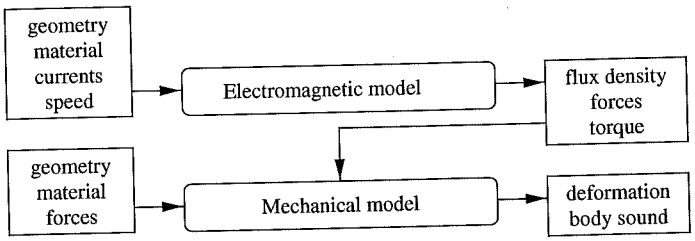

Figure 1.
Computational two-step chain

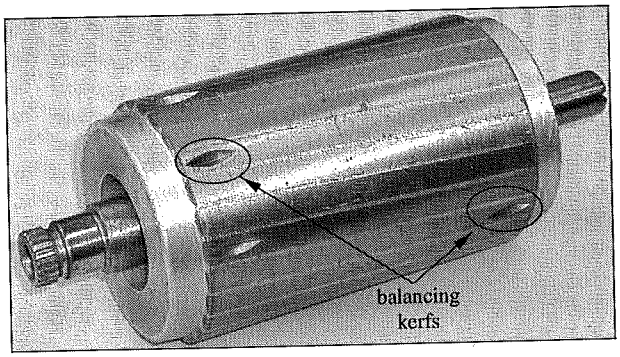

Figure 2.
Rotor of IM with balancing kerfs

2. Electromagnetic simulation

In order to estimate the worst case configuration the maximum size of the balancing kerfs is considered for the electromagnetic, 2D finite-element model. Figure 4 shows the section of the rotor containing the kerfs. As a reference a model without kerfs is applied. Both models are simulated with a transient solver (van Riesen *et al.*, 2004). The model is simulated at nominal speed $n = 1{,}200\,\mathrm{min}^{-1}$ and at stator frequency of $f_1 = 48.96\,\mathrm{Hz}$. For each of the $N = 2{,}056$ time steps simulated the flux-density distribution is provided. From this the torque and the surface-force density on the stator teeth are derived (Jordan, 1950; Schlensok and Henneberger, 2004; Timar, 1989).

The analysis of the air-gap flux-density shows that the "balanced" model generates extra pole-pair numbers (Figure 5). The four-pole IM with $N_S = 36$ slots in the stator and $N_R = 26$ in the rotor now has odd numbers showing the dynamic eccentric impact of the balancing kerfs to the machine's behaviour. Nevertheless, the most significant occurring pole-pair numbers ν are:

$$\nu = p = 2 \tag{2}$$

$$\nu = N_R \pm p = 24, 28 \tag{3}$$

$$\nu = N_S \pm p = 34, 38. \tag{4}$$

For the analysis of the torque the results of the two models are combined, since the balancing kerfs only affect an axial portion of the rotor (about 17 per cent of the

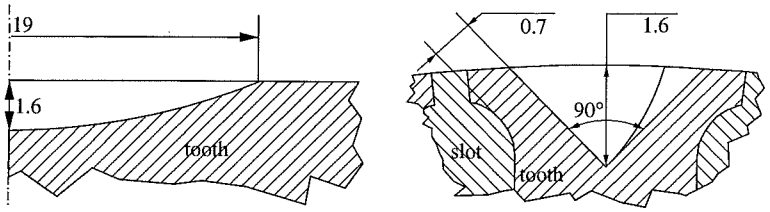

(a) Longitudinal section. **(b)** Cross section.

Figure 3.
Maximum measures of the balancing kerf

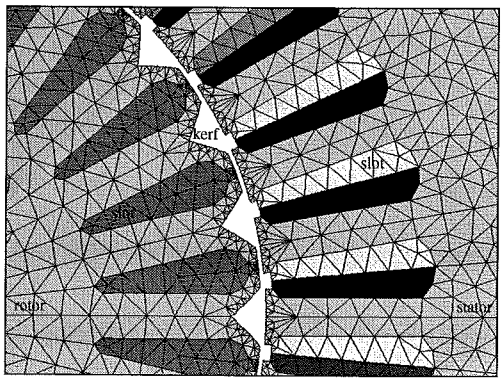

Figure 4.
FE-model of IM with maximum worst-case balancing kerfs

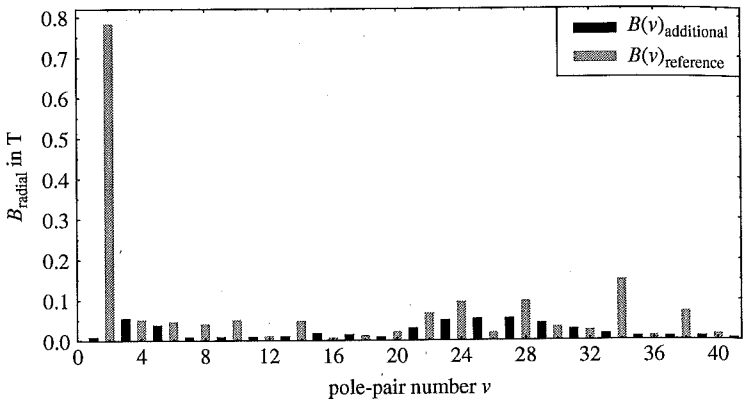

Figure 5.
Pole-pair numbers of the air-gap flux-density of both models

armature length on each end of the rotor). Therefore, the torque is averaged. 66 per cent are taken from the reference model and each 17 per cent of a model with kerfs depending on their location on the circumference. There are 13 models, since the kerfs on both ends can be shifted against each other. For the calculation of the torque in fact a modified multi-slice models (Gyselinck *et al.*, 2001) is applied as Figure 6 shows in brief. The axial length of the rotor l_z is assigned to $i = 1 \ldots 5$ slices with the individual axial length of $l_z \cdot \eta_i$ according to a weight of γ_i. In order to exclude other effects skewing has been neglected in the FEM-model.

The multi-slice model results in a rather small impact to the torque behaviour decreasing the average torque by about 1.4%. However, balancing results for the studied IM in high-net forces of about $F = 23$ N acting onto the bearings. Therefore, the analysed IM is no longer balanced. The resulting un-balanced fugal forces are smaller than the net forces produced by balancing. Owing to symmetry the net force of the reference model can be neglected.

As the analysis of the surface-force density σ on the stator teeth shows the balancing kerfs have some local effect to the force excitation of the IM. Figure 7 shows the surface-force density-excitation for the same stator teeth and the same time step for both models. It is stated that the kerfs generate some extra force peaks and raise the amplitude of already existing harmonics. Since, the kerfs rotate with the rotor this results in a modulation of the surface-force density-spectrum shown in Figure 8 (Jordan, 1950; Schlensok and Henneberger, 2004). Next to this, the σ is raised for the regions of the stator teeth in the range of the kerfs throughout the spectrum.

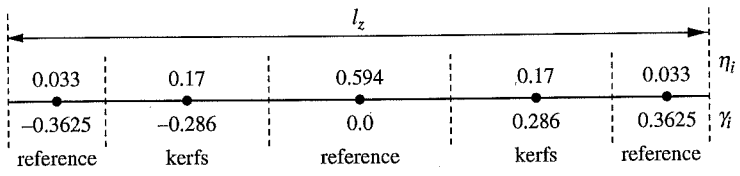

Figure 6.
Multi-slice model for torque and structure-dynamic simulation

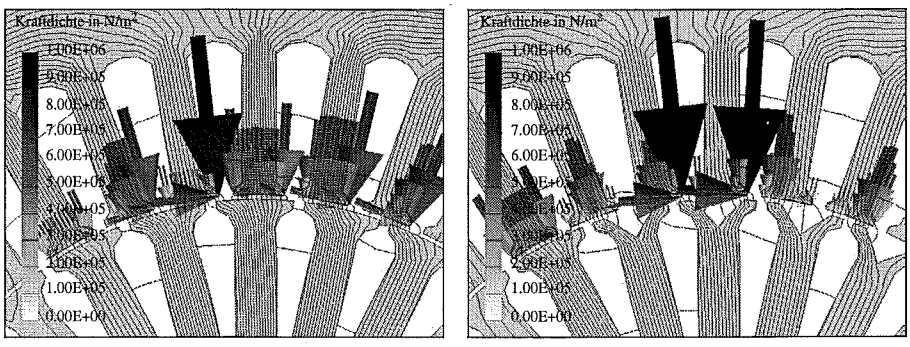

Figure 7.
Surface-force density for both models at same time step

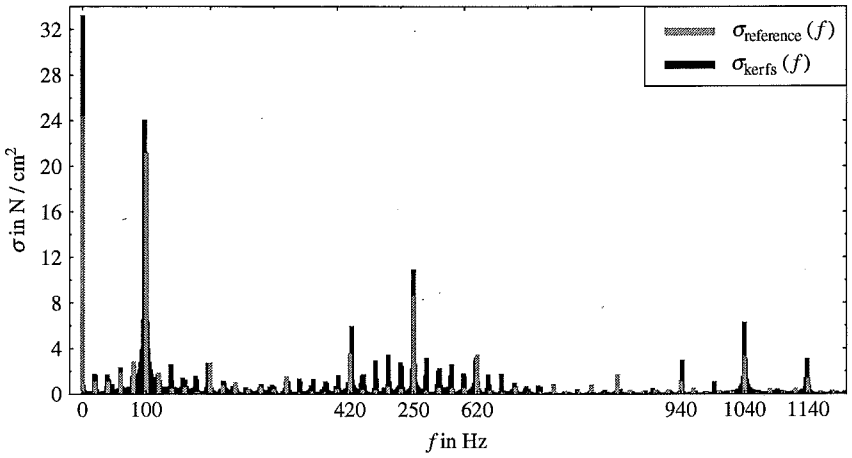

Figure 8.
Spectrum of the surface-force density modulated with rotor speed

3. Structure-dynamic simulation

In the next step, the mechanical, structure-dynamic behaviour of the IM is studied to estimate the impact of the balancing kerfs. Therefore, a mechanical model is applied (Schlensok *et al.*, 2006) which consists of all mechanical parts of the IM, such as stator, rotor, shaft, housing, bearings, and housing caps (Figure 9). The IM is mounted on the front plate. Hence, the rear part of the machine can oscillate freely.

For the analysis of the vibrations of the IM the surface-force density derived from the electromagnetic model is transformed to the frequency domain and than for each

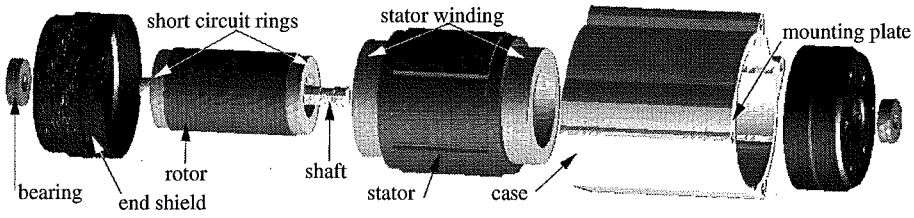

Figure 9.
Exploded view of the structure-dynamic model of the IM with squirrel-cage rotor

regarded frequency to the mechanical model. Significant frequencies are the slot harmonics of stator and rotor. The rotor-slot harmonic is modulated with the double stator frequency. Finally, the rotor speed has to be considered due to the dynamic-eccentric effect of the balancing kerfs. The studied frequencies are: $f = 20$, 98, 422, 520, 618, 720, 942, 1,040, and 1,138 Hz. For these frequencies the force excitations of four different electromagnetic models are taken into account: reference model, model with kerfs only on front end of rotor, model with kerfs on rear end, and model with kerfs on both ends.

The force transformation applies the 2D multi-slice model from the electromagnetic simulation described above (Figure 6). With a novel method the forces are transformed from the slices to the ranges of the stator of the mechanical model assigned to the corresponding slice. By this, higher resolutions in the frequency and space domains are reached in comparison to an equivalent 3D, electromagnetic model. Figure 10 shows the procedure of transformation. For 3D, mechanical elements which show an overlapping of force assignment the value of σ is averaged. This is the case for element 6. The force of slice 2 is weighted with a and of slice 3 with b.

A 3D, electromagnetic FE-model would afford by far more elements and would result in an unreasonable computing duration if the same resolution of the spectrum should be reached ($\Delta f = 2$ Hz at a cut-off frequency of $f_{co} = 1{,}200$ Hz). As own studies have shown the applied novel method results in more accurate results of the structure-dynamic model when compared to measurements of the body-sound level.

After simulation of the mechanical model by applying the 13 different balanced and the reference model in the electromagnetic force calculation, the deformation is analysed in three different ways.

3.1 Deviation of the deformation

In a first step, the deviation of the deformation is analysed. This principle subtracts the deformation values of all nodes of the model considering the results of a balanced and the reference model. Therefore, positive values show regions of higher deformation of the balanced model and negative values consider higher values for the reference model.

Figure 11 shows exemplarily the difference of the deformation for $f = 1{,}040$ Hz of housing and stator. Here, balancing kerfs on both ends of the rotor are compared to the reference model. Similar to a dynamic-eccentric rotor the balancing kerfs result in higher deformation of the complete structure. Especially, the rear (free) end of the IM oscillates stronger (dark regions in figure). Independent of which balanced model is regarded, this effect can be stated.

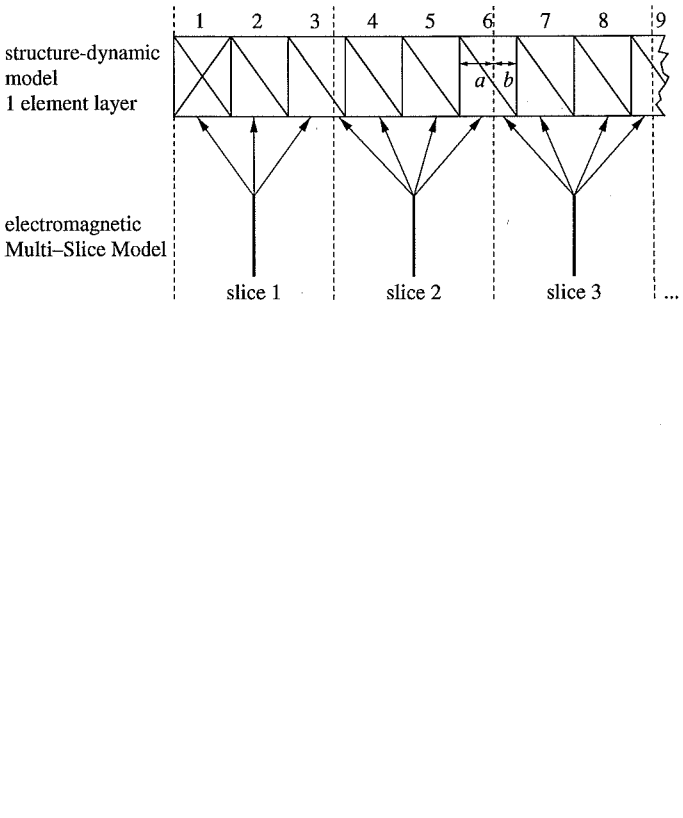

Figure 10.
Principle of force transformation

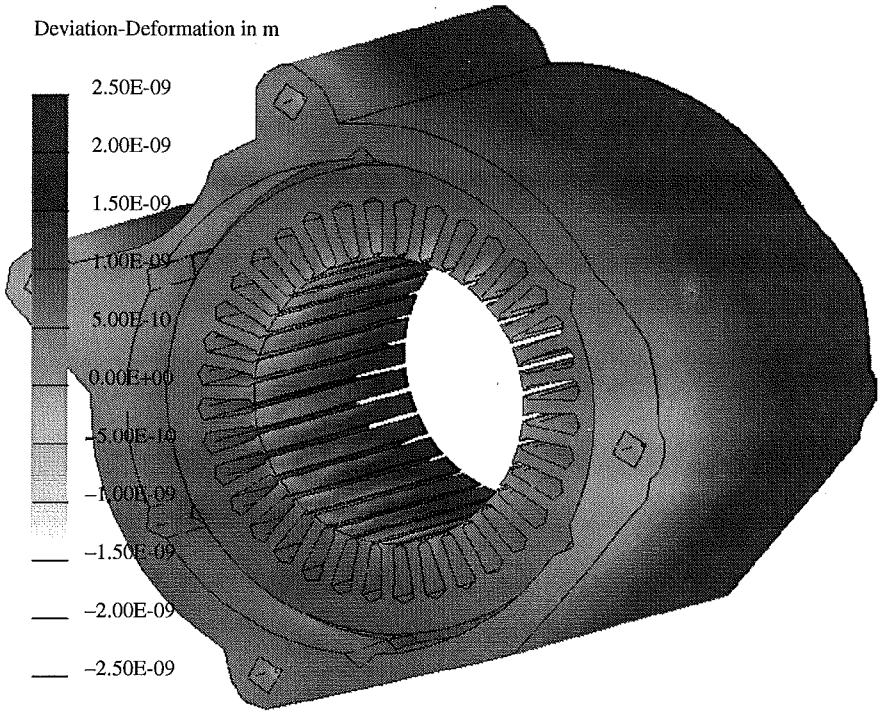

Figure 11.
Example: deviation of the deformation: $f = 1{,}040$ Hz

3.2 Body-sound index

The second analysis scheme is the level of the body-sound index L_{BSI}. The L_{BSI} is an integral value of the deformation of an entire body for instance the housing of the IM. For the nodes of all elements p of the body the normal component of the velocity of deformation $\vec{v}_p$ is summed up. The sum is related to the reference values $S_0 = 1\,\mathrm{m}^2$ and $h_{U_0}^2 = 25 \times 10^{-16}\, m^2/s^2$ and the level is calculated:

$$L_S(f) = 10\ \log\left(\frac{\sum_{p=1}^{N_{el}} \int_{S_p} |\vec{v}_p \cdot \vec{n}^p|^2 \mathrm{d}S}{S_0 \cdot h_{U_0}^2}\right). \tag{5}$$

$\vec{n}^p$ is the normal vector of the element p, f is the frequency and N_{el} the number of elements. Therefore, the L_{BSI} allows for the global evaluation, analysis, and comparison of a body's entire deformation. The L_{BSI} is a pure computational value and can therefore not be compared to any measurement.

The body sound of the housing can be transmitted to other parts of the mechanical construction, i.e. the mounting. Therefore, the L_{BSI} of the housing is studied. Figure 12 shows the results for four models, i.e. the reference model, a model with kerfs on the front and on the rear end of the rotor, and a model each with kerfs on one of both ends. As the studies show, the models with kerfs on both ends of the rotor show a weak dependence on the relative location between the kerfs on each end. Therefore, studying only the model with kerfs on both ends is sufficient.

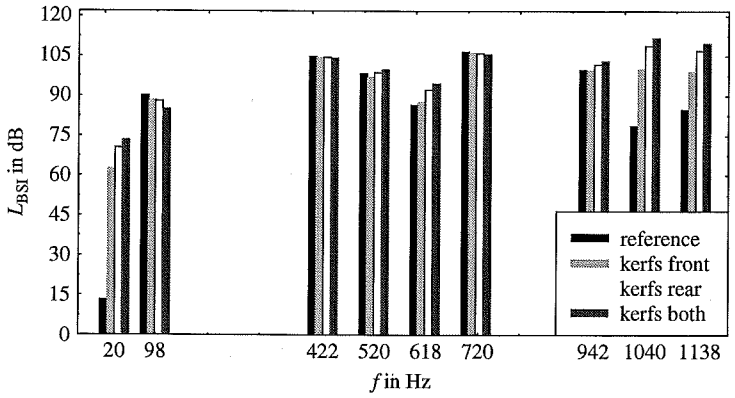

Figure 12.
Body-sound index of the IM's housing

Except for $f = 98$, 422, and 720 Hz the balancing kerfs rise the level of the body index sound of the housing. Especially the higher frequencies studied at $f = 1{,}040$ and 1,138 Hz increase by up to 35 dB. For rotor speed at $f = 20$ Hz the level is increased up to 60 dB. But being very low for the reference model this order keeps smallest in the spectrum also for the balanced models. Figure 13 shows the difference in the L_{BSI} of the balanced models compared to the reference model.

3.3 Body-sound level

Finally, the body-sound level L_{BS} allows for local analysis of the vibration. The L_{BS} is a local value. Therefore, a global analysis as for the L_{BSI} is not possible. Figure 14 shows the analysis lines and the positioning of the acceleration sensor used for measurements. Along the analysis lines the deformation is sampled and the body-sound level is calculated by:

$$L_S = 20 \cdot \log \frac{a}{1(\mu\text{m/S}^2)} \text{dB}. \tag{6}$$

a is the acceleration of the specific node at the regarded frequency f. As an example the radial component of the L_S is studied for both analysis lines on the housing for

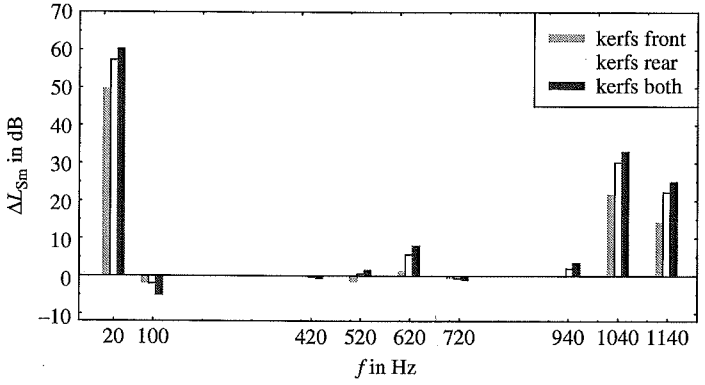

Figure 13.
Difference of body-sound index of the IM's housing

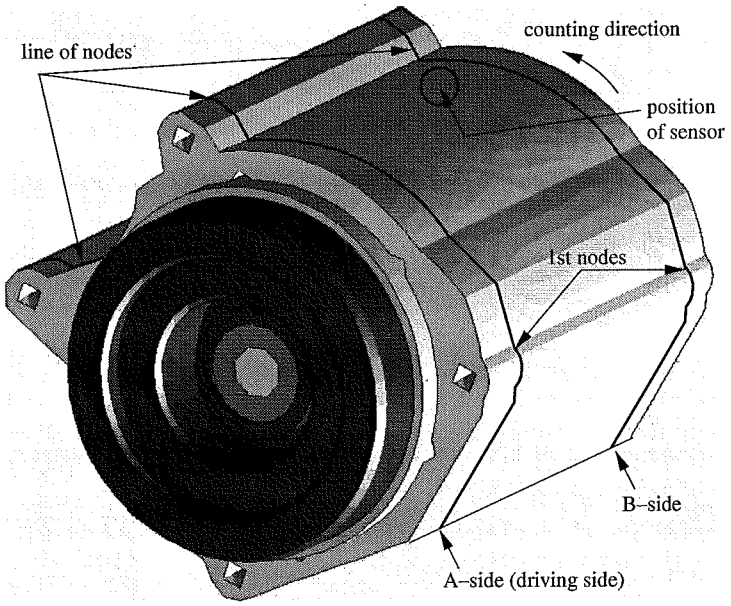

Figure 14.
Analysis lines and positioning of sensor for the body-sound level

$f = 422$ Hz for models with kerfs on either end of the rotor (Figure 15). The L_S oscillates strongly on the front end of the IM. This is due to the mounting which is performed by fixing the edges of the drilling holes on the front end of the mounting plate in the housing. This results in the four minima shown in Figure 15. The six maxima stem from the coupling of stator and housing by six spiral-steel springs. The stator's deformation is transmitted just by the six spiral spring pins which fix the stator in the housing (Figure 9). On the freely oscillating rear end of the IM the L_S is higher and is rather independent on the mounting and the coupling of stator and housing.

The analysis of the L_S at the location of the acceleration sensor shows a similar result as for the body-sound index. Figure 16 exemplarily sums up the results for all variants studied for the radial component of the body-sound level. The levels for higher

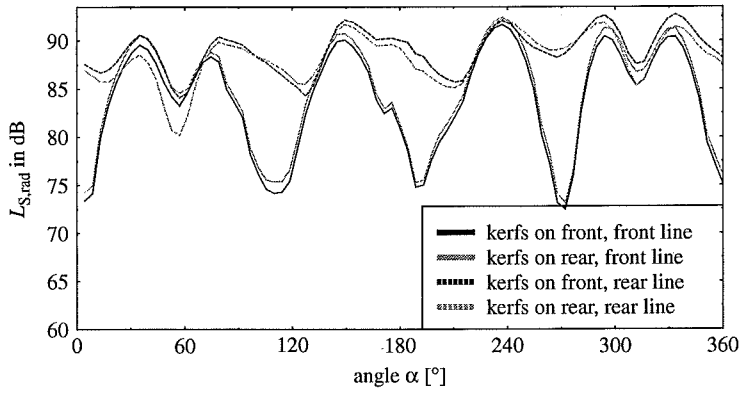

Figure 15.
Body-sound level along analysis lines for $f = 422$ Hz

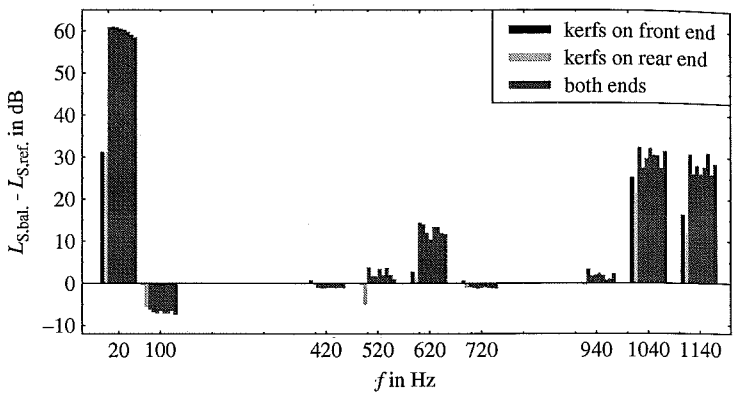

Figure 16.
Body-sound level at sensor location

orders and for rotor speed increase strongly especially for the case of balancing kerfs on both ends of the rotor. Next to these orders the 31 harmonic at $f = 618$ Hz increases in the case of balancing kerfs significantly.

4. Conclusions

The presented studies and simulation results show the potential of the structure-dynamic simulation chain for improvement and verification of the design of electrical machines. Here, the impact of balancing kerfs on the rotor of an IM is analysed. In general, the applied methods can be used for the analysis and optimization of any kind of manufacturing or tolerance problem of electrical machines such as various kinds of eccentricity, punching kerfs, broken bars, magnetization errors in permanent-magnet machines, and others.

As a result of the studies presented in this paper the analysed IM is no longer balanced. The resulting un-balanced fugal forces are smaller than the net forces produced by balancing. Without balancing the IM induces less body-sound to the mechanical system of the application and the IM is hardly excited at rotor speed. For rotor speed (first order) the balancing kerfs result in strongly increasing body sound, i.e. vibration and mechanical stress. At frequencies above $f = 1{,}000$ Hz the body sound rises significantly as well. This frequency range is critical since the human ear is very sensible here. Hence, the IM will be experienced more noisy. From this result, the IM is no longer balanced in series production. This leads to a major economic benefit.

References

De Gersem, H., Ion, M., Wilke, M., Weiland, T. and De-menko, A. (2006), "Trigonometric interpolation at sliding surfaces and in moving bands of electrical machine models", *COMPEL*, Vol. 25 No. 1, pp. 31-42.

Gyselinck, J.J.C., Vandevelde, L. and Melkebeek, J.A.A. (2001), "Multi-slice FE modelling of electrical machines with skewed slots – the skew discretization error", *IEEE Trans.-Mag.*, Vol. 37 No. 5, pp. 3233-7.

Jordan, H. (1950), *Geräuscharme Elektromotoren*, Verlag W. Girardet, Essen.

Lingener, A. (1992), *Auswuchten – Theorie und Praxis*, Verlag Technik GmbH, Berlin.

Schlensok, C. and Henneberger, G. (2004), "Comparison of static, dynamic, and static-dynamic eccentricity in induction machines with squirrel-cage rotors using 2D-transient FEM", *COMPEL*, Vol. 23 No. 4, pp. 1070-9.

Schlensok, C., van Riesen, D., Küest, T. and Henneberger, G. (2006), "Acoustic simulation of an induction machine with squirrel-cage rotor", *COMPEL*, Vol. 25 No. 2, pp. 475-86.

Timar, P.L. (1989), *Noise and Vibration of Electrical Machines*, Elsevier, Amsterdam.

van Riesen, D., Monzel, C., Kaehler, C., Schlensok, C. and Henneberger, G. (2004), "iMOOSE – an open source environment for finite-element calculations", *IEEE Trans.-Mag.*, Vol. 40 No. 2, pp. 1390-3.

About the authors

C. Schlensok received the MSc degree in Electrical Engineering in 2000 from the Faculty of Electrical Engineering and Information Technology at RWTH Aachen University Germany. From 2001 to 2006, he has been researcher at the Institute of Electrical Machines at RWTH Aachen University. In 2005, he obtained the PhD degree at the Faculty of Electrical Engineering and Information Technology at RWTH Aachen University with a thesis on numeric simulation and optimisation of induction machines. With the beginning of 2007, he moved to industry to Bosch Rexroth AG in Lohr am Main, Germany. He is now responsible for the design, calculation, and simulation of induction and synchronous machines as well as torque and linear motors. He is member of the developer team for the finite-element software iMoose (www.imoose.de). C. Schlensok is the corresponding author and can be contacted at: Christoph. Schlensok@boschrexroth.de

K. Hameyer (Senior MIEEE, Fellow IET) received the MSc degree in electrical engineering from the University of Hannover, Germany. He received the PhD degree from University of Technology Berlin, Germany. After his university studies, he worked with the Robert Bosch GmbH in Stuttgart, Germany, as a Design Engineer for permanent magnet servo motors and board net components. In 1988, he became a Member of the Staff at the University of Technology Berlin, Germany. From November to December 1992, he was a Visiting Professor at the COPPE Universidade Fderal do Rio de Janeiro, Brazil, teaching electrical machine design. In the frame of collaboration with the TU Berlin, he was in June 1993 a Visiting Professor at the Université de Batna, Algeria. Beginning in 1993, he was a Scientific Consultant working on several industrial projects. Currently, he is a Guest Professor at the University of Maribor in Slovenia, the Korean University of Technology and Education (KUTE) in South-Korea. He was awarded his Dr habil. from the Faculty of Electrical Engineering of the Technical University of Poznan, Poland, and was awarded the title of Dr h.c. from the Faculty of Electrical Engineering of the Technical University of Cluj Napoca, Romania. Until February 2004, he was a Full Professor for numerical field computations and electrical machines with the K.U. Leuven, Belgium. Currently he is the Director of the "Institute of Electrical Machines" and holder of the Chair "Electromagnetic Energy Conversion" of the RWTH Aachen University, Germany (www.iem.rwth-aachen.de/). Since 2007 he is dean of the faculty of electrical engineering and information technology at RWTH Aachen, Germany. His research interests are numerical field computation, the design of electrical machines, in particular permanent magnet excited machines, induction machines and numerical optimisation strategies. He is author of more than 100 journal publications, more than 200 international conference publications and author of four books.